sciendo

Műszaki Tudományos Közlemények vol. 12. (2020) 55–62.
DOI: English: https://doi.org/10.33894/mtk-2020.12.08
Hungarian: https://doi.org/10.33895/mtk-2020.12.08

EME MTSZ MTK

NUMERICAL EVALUATION OF THE SHAPER CUTTER WITH CYLINDRICAL RAKE FACE

Márton MÁTÉ,[1] Dénes HOLLANDA [2]

Sapientia Hungarian University of Transylvania, Faculty of Technical and Human Sciences, Department of Mechanical Engineering, Târgu-Mureș, Romania

[1] *mmate@ms.sapientia.ro*

[2] *hollanda@ms.sapientia.ro*

Abstract

This paper deals with the geometric built-up of a theoretically profile errorless shaper cutter. Its proposed rake face is a cylindrical surface for each tooth. The setting parameters of this are the axis inclination angle and the grinding wheel's radius. The possible domain of the setting parameters is computed from geometrical restrictive conditions. The proposed numerical evaluation consists in the computing of the orthogonal rake angle variation, together with the deviation of the generating pro-file from the perfect involute. The obtained results allow the formulation of some conclusions regarding the influence of the cylinder radius and the axis inclination: the best rake angle distributions are obtained when using increased radius values, while profile deviation becomes minimal when using smaller radii and axis inclination angles.

Keywords*: shaper cutter, rake face, rake angle, distribution, profile error.*

1. An overview of the right toothed shaper cutter with cylindrical rake face

As is well known, shaper cutters have a theoretical profile error. In order to keep this error within the limits of profile tolerance, the classical solution recommends the utilization of small constructive addendum rake- and relief angles [1, 2]. The rake face and the addendum relief face of a classical straight toothed shaper cutter are circular cones, with axes coincident to the axis of the shaper cutter. They provide a poor top geometry resulting from $\gamma_V = 5°$ and $\alpha_V = 6°$. As a consequence, the side rake angle barely reaches the value of 2° in the edge tip, and decreases with the radius of the edge point.

The advantage of the shaper cutter model proposed in the present paper is the significant improvement of the chip forming conditions on the side edges. Moreover, the theoretical profile error reduces to zero in the case of the new cutting tool, and it rises by only negligible values as the shaper cutter reaches the last re-sharpening or the total wear stage. The profile error magnitude here is several times smaller than in case of the classic tool.

The fundamental difference between the classic solution and the proposed one rests in the method for generating the tooth's flank surfaces: the geometric built-up of the shaper cutter tooth starts from the generating wheel, not from the generating rack. The detailed mathematical description of the model [3] is based on the following geometrical principles:

- the generating wheel is a gear with the same tooth number as the shaper cutter, and a maximum possible profile shifting, allowed by the condition of minimum necessary topland width;
- the rake face is a cylinder with radius ρ_p whose axis closes the angle γ_a with a plane perpendicular to the shaper cutter's axis;
- the side edges result as intersections between the tooth flanks of the generating wheel and the rake face;
- the side relief faces of the shaper cutter's tooth are helical surfaces whose helix parameter is computed from the side relief angle value. They

result through roto-translations of opposite senses but same helix parameter of the side edges.

The generating wheel tooth's flanks and the incident side edges are shown in **Figure 1.**

It can be observed that the z coordinates of the edges raise barely out of the horizontal plane $(x_s y_s)$ of the involute profile. The rake angles are significantly greater than in the case of the classic shaper cutter.

Figure 2. presents the flanks of the shaper cutter and the rake face. The helix parameter was computed for a side relief angle value of 2°.

Figure 2. shows the rake face in two positions: the netted grey position result as a translation along the z axis and corresponding to the final wear state of the cutter.

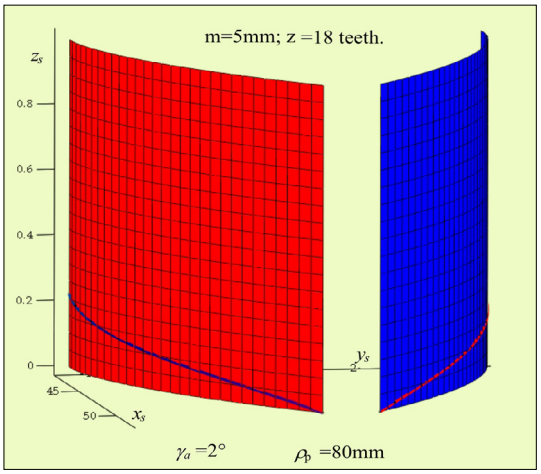

Figure 1. *The flanks of the generating wheel tooth and the side edges of the shaper cutter*

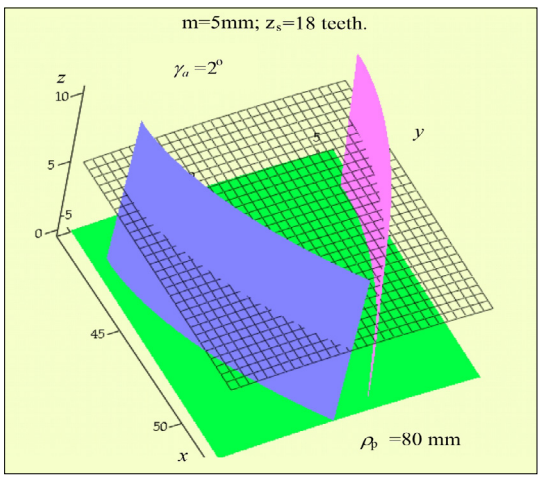

Figure 2. *The side relief faces and the rake face*

2. The rake face setting limits

Mathematically it can be stated that the two independent parameters of the rake face produce a double infinite manifold of surfaces. From this must be chosen the technically possible solutions. When defining the restrictive conditions, two aspects were considered:

- the intersection curve of the cylinder and the generating wheel's tooth flank must extend to the whole height of the tooth;
- the rake angle on the tip of the lateral edge equals the value determined from the cutting conditions.

A qualitative inspection of the reciprocate position of the involved geometrical elements led us to conclude that the first condition returns the minimum possible value of the radius, while the second limits the axis inclination value. The calculus is fully presented in **[3]**. The first restriction is primed through the following inequality:

$$\sqrt{\rho_p^2 - \left(\sqrt{\rho_p^2 - \frac{s_a^2}{4}} - \Delta H_c \sin\gamma_a\right)^2} \geq y_C$$

$$y_C = R_b \sin\varepsilon - \left(R_b\, tg\,\alpha_t + \rho_f\right)\cos\varepsilon + \rho_f \cos(\psi_1)$$

$$\rho_f = \frac{R_t^2 - R_f^2}{2\left(R_f - \sqrt{R_t^2 - R_f^2}\right)} \qquad (1)$$

$$\angle BOC$$

$$\psi_1 = \mathrm{tg}\,\alpha_t - \eta + \arcsin\frac{R_b}{R_f + \rho_f}$$

In formula (1) index t refers to the involute's beginning circle while index f refers to the dedendum circle. The root fillet is approximated to a circle arch of radius ρ_f **[4]**, **[6]**.

The second restriction defines a relation between the radius ρ_p and the axis inclination angle γ_a:

$$\mathrm{tg}\,\gamma_{Oa} = \mathrm{tg}\,\gamma_a \sin\psi + \frac{s_a}{2\sqrt{\rho_p^2 - \frac{s_a^2}{4}}}\frac{\cos\psi}{\cos\gamma_a} \qquad (2)$$

$$\psi = \mathrm{tg}\,\alpha_a - \eta$$

Restriction (1) was grouped on the form $F_1 = 0$ and studied for a particular case defined by a shaper cutter of module = 5 mm , teeth number Z_s = 18 and the rake face's independent parameters $\gamma_a \in [2°,10°]$ and $\rho_p \in [20,100]$. **Figure 3.** shows the surface of F_1 values.

The limit curve is defined by the intersection of the F_1 surface and the plane of level zero. It de-

fines the border of the domain of the possible ordered pairs (γ_a, ρ_p). As **Figure 3.** shows, this is the the half-plane not containing the origin.

The coordinates of several points on the limit curve were numerically computed. For this, a number of N = 30 equidistant values were taken on the interval of the axis inclination angle γ_a. Every angle value was associated with the minimum possible value of the radius. This radius value is increased with a given ratio until the following inequality occurs:

$$F_1(\gamma_a, \rho_{pmin})\, F_1(\gamma_a, \rho_{pmin} + \delta_\rho) < 0 \qquad (3)$$

Once achieving the interval (ρ_p, $\rho_p + \delta_p$), the radius limit value is computed through the method of chords with a precision of 10-4. The limit curve is represented in **Figure 4.**

The second restrictive condition, by setting a given orthogonal rake angle value in the tip of the edge allows us to compute the corresponding ordered pairs (γ_a, ρ_p) In order to facilitate the computation, the limit curve will be defined using two spline functions, defined on the system of the N=30 nodes computed previously:

$$\gamma_a(\rho_p) = \mathrm{Sp}_1(\rho_p)$$
$$\rho_p(\gamma_a) = \mathrm{Sp}_2(\gamma_a) \qquad (4)$$

The technologically acceptable orthogonal rake angle values are considered in the interval $\gamma_{Oa} \in [3°, 9°]$ and considered in 30 equidistant points.

In order to gain the possible ρ_p values for any γ_{Oa} value, equation (2) will be rearranged. Priming the radical expression, and imposing its firm positivity, the following constraint is obtained:

$$\mathrm{tg}\,\gamma_{Oa} - \mathrm{tg}\,\gamma_a \sin\psi > 0 \qquad (5)$$

With this equation, the maximum possible value of axis inclination angle is computed. The minimum acceptable value is established considering technological reasons. Now any value of γ_{Oa} from the interval of N = 30 equidistant values is considered. For each of them, any possible γ_a axis inclination angle is taken into consideration, which determines, on the basis of equation (2), the corresponding ρ_p value. In this way, any ordered pair (γ_a, ρ_p) , for a given γ_{Oa} is computed. A very suggestive geometrical representation can be made here, putting on the *z*-axis the imposed rake angle values. For each value corresponds a level curve $F(\gamma_a, \rho_p; \gamma_{Oa}) = 0$. It results, that a given rake angle value in the tip of the side edge is realizable through an infinite number of combinations of radiuses and axis inclination angles. The contour plots and the limit curve is represented in **Figure 5.**

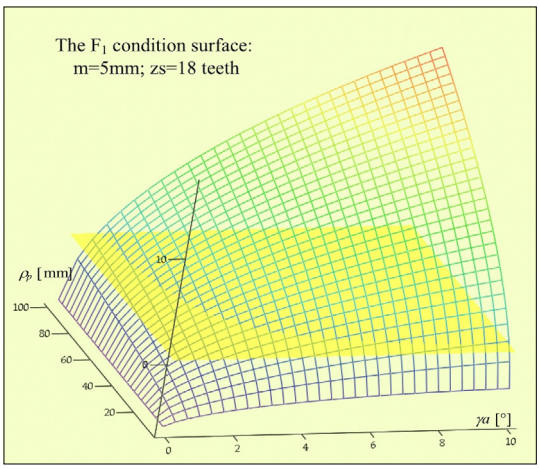

Figure 3. *The surface attached to the condition F1*

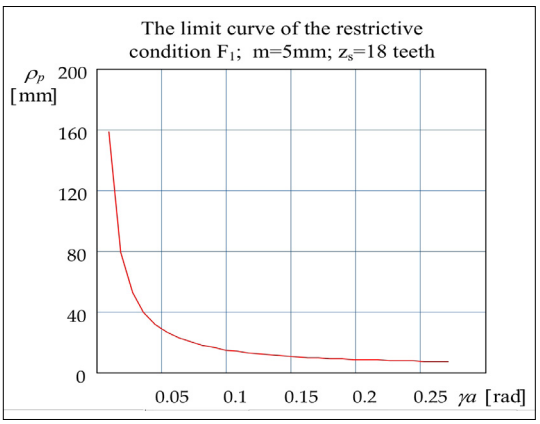

Figure 4. *The limit curve derived from restrictive condition F_1*

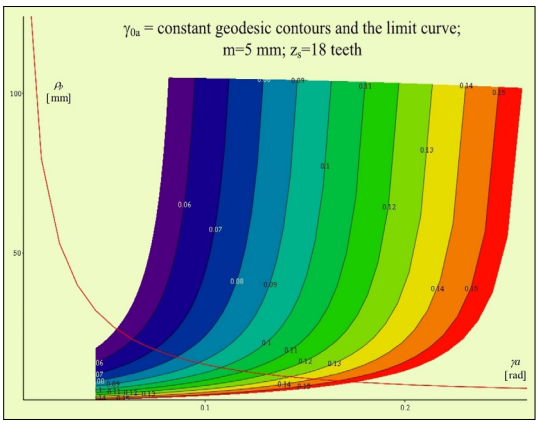

Figure 5. *Contour plots of γ_{Oa} = const. and the limit curve*

3. The variation of the side relief angle

Let's suppose the equations of the rake face, the cutting edge and the flank (the relief face) are known. With these, the tangent of the edge and the normal of the rake face can be deter-mined for each edge point. Next to these the basis of the tool-in-hand frame can be computed. Using all quantities mentioned, the rake angle vector expression is given by [5], [7], [8]:

$$\sin\gamma_O = \frac{\mathbf{n}_\gamma \cdot \mathbf{j}}{|\mathbf{n}_\gamma \times \mathbf{i}|} \tag{6}$$

The vectors of the expression above are shown in Figure 6. The tool-in-hand frame is fixed in the arbitrary M point of the cutting edge, where the basis vectors **k**, **j** and **i** are respectively the unit normal vectors of the basic, the tangent and the orthogonal measuring plane. $\boldsymbol{\tau}$ is the tangent vector of the edge curve in M and $\mathbf{n}_\gamma$ the rake face's normal vector. The detailed calculus of these can be found in [3]. All vectors are primed in a frame centered on the symmetry plane of the generating wheel's tooth: axis z is the axis of the wheel, axis x the axis of the involute tooth profile and the y axis is perpendicular to both of these. The necessary vector expressions are as follows:

$$\mathbf{k} = (0 \quad 0 \quad -1)^T \tag{7}$$

$$\mathbf{j} = \frac{\mathbf{k} \times \boldsymbol{\tau}}{|\mathbf{k} \times \boldsymbol{\tau}|} \tag{8}$$

$$\mathbf{i} = \mathbf{j} \times \mathbf{k} \tag{9}$$

$$\boldsymbol{\tau} = \left(\frac{\partial F_h}{\partial x} \quad \frac{\partial F_h}{\partial y} \quad \frac{\partial F_h}{\partial z}\right)^T \tag{10}$$

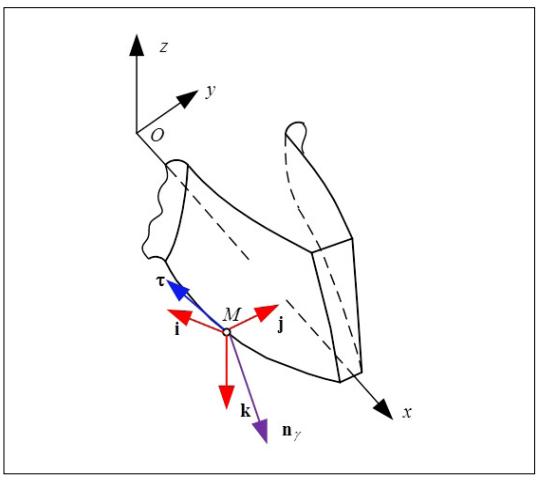

Figure 6. *The vectors involved in the computing of the rake angle*

Notation F_h in equation (10) is used for the implicit expression of the cylindrical rake face.

The repartitions of the rake angle values along the cutting edge, in dependence with the cylinder's axis inclination and radius are presented in the next.

The simulation was performed inside the domain $\gamma_a \in [2°, 5°]$ and $\rho_p \in [\rho_{pmin}, 100]$ for the following ordered pairs:

$\{2°; 3°; 4°; 5°\} \times \{\rho_{pmin}; 40; 60; 80; 100\}$

The value ρ_{pmin} is inversely proportional to the inclination angle γ_a.

Figure 7. shows the rake angle repartition surfaces. The shape and the relative position of the surfaces permits the identification of the following peculiarities:

- the limits of the variation interval of the rake angle raise with the decrease of the radius of the cylinder;
- the variation interval of the rake angle increases tith the decrease of the radius of the cylinder ;
- the repartition along the edge is approximately parabolic.

The variation of the rake angle is detailed in Figure 8, 9, 10 and 11.

The repartitions were examined also from statistical point of view. The average values of repartition are shown in Figure 12.

As mentioned before, the minimum cylinder radius values depend on the axis inclination angle. There exists axis inclination values for which the minimum radius value of the considered interval is not applicable. In such points the average value was conventionally considered zero. The visual inspection of non-zero values shows that the rake angle average value increases with the axis inclination angle and decreases with the radius of the cylinder.

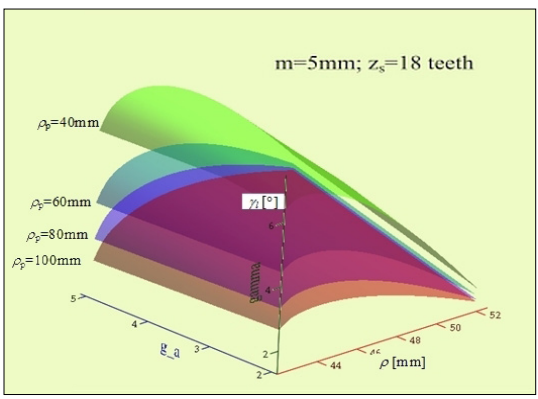

Figure 7. *The rake angle repartition surfaces along the cutting edge*

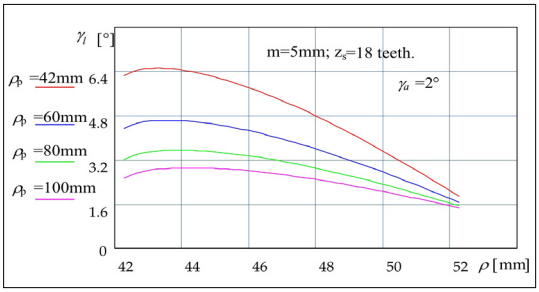

Figure 8. *Rake angle repartition for an axis inclination of 2°*

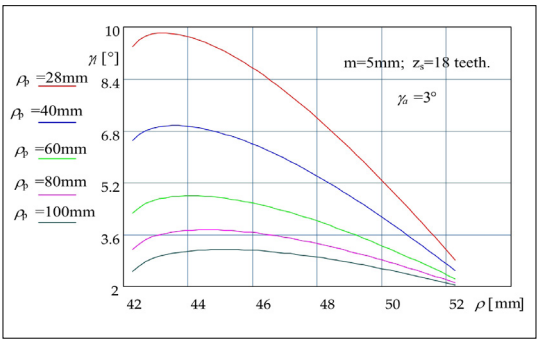

Figure 9. *Rake angle repartition for an axis inclination of 3°*

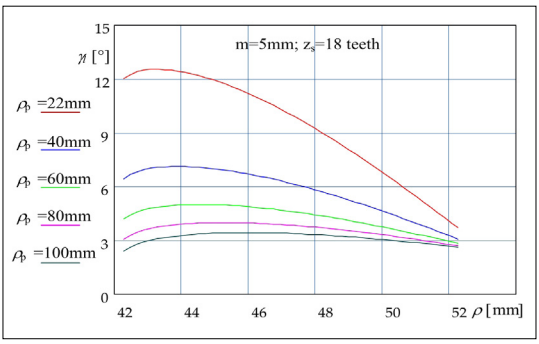

Figure 10. *Rake angle repartition for an axis inclination of 4°*

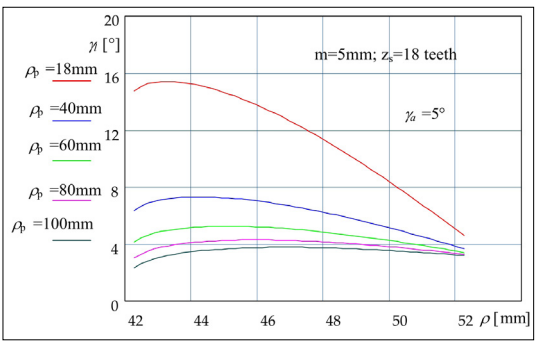

Figure 11. *Rake angle repartition for an axis inclination of 5°*

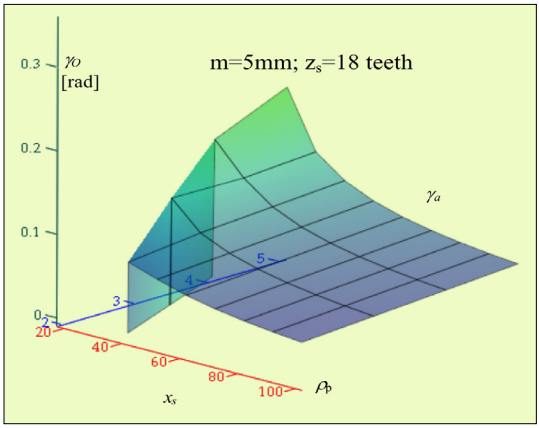

Figure 12. *Rake angle average values repartition*

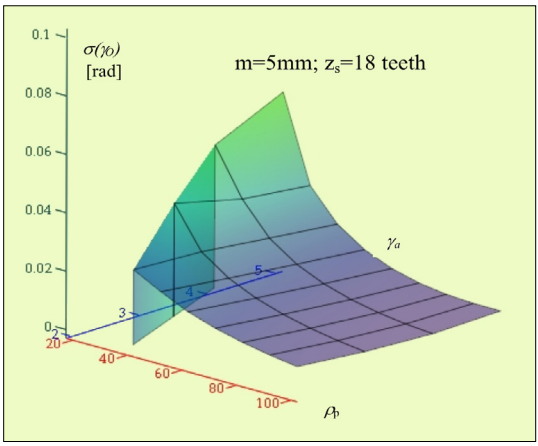

Figure 13. *The map of the rake angle standard deviation*

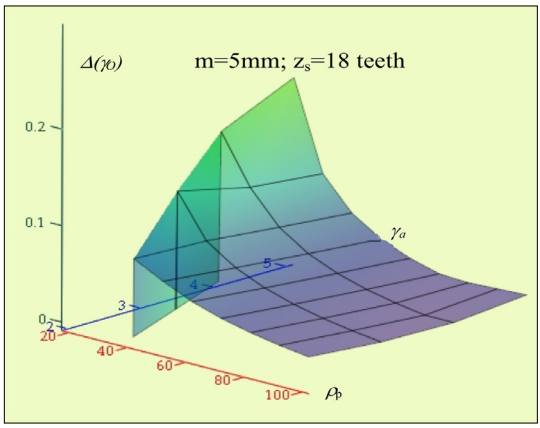

Figure 14. *The repartition of the amplitude of the rake angle variation interval*

The repartition of the standard deviation is presented in **Figure 13.** It can be easily observed that standard deviation follows the same variation

type as the average. Thus, greater average values are accompanied by greater standard deviation too. Equivalent information to the standard deviation map offers also the repartition of the amplitudes of the variation intervals. This is shown on **Figure 14.**

The amplitude surface shows a local minimum in the domain defined by $\gamma_a \in (4°, 6°)$ and $\rho_p \in (80, 100)$. Otherwise the amplitude of the variation interval increases with the axis inclination angle while it decreases with the radius of the cylinder.

4. The tooth profile

In the case of the proposed shaper cutter construction two tooth profiles have to be defined: the tool tooth profile and the tool's generating profile. The tool tooth profile results from the intersection between the flanks of the shaper tooth (the side relief faces) with a plane perpendicular to the cutter's axis. The tool's generating profile is, by definition, the profile of the tooth meshed by the cutting edges, during the main cutting motion (here a vertical linear translation). The technological meshing of the tooth flanks is based on the principle of coupling between a rack and a gear. Different analytical description of this geometric-kinematic phenomenon is fully described in **[6]**, **[9]**, **[10]**, **[11]**]. If the tool tooth profile deviates to an unacceptable extent from the theoretically perfect involute, the grinding of the flanks becomes impossible with a straight profiled grinding wheel. In such cases the shaper cutter tooth height must be variable. If the deviation of the tool tooth profile from the involute is less than the amplitude of the manufacturing errors, the grinding can be performed using the Maag or the Niles principle, and it results in a shaper cutter with constant tooth height.

The tool tooth profile is computed on the base of the parametric coordinate functions of the cutting edge and the helix parameter of the relief face. The geometric quantities are shown of **Figure 15.**

Lets consider the parametric equations of the new (never re-sharpened) shaper cutter edge as the intersection of the flank of the generating wheel and the circular cylinder of the rake face:

$$\begin{cases} x(\varphi) = R_b(\cos(\varphi-\eta) + \varphi\sin(\varphi-\eta)) \\ y(\varphi) = jR_b(\sin(\varphi-\eta) - \varphi\cos(\varphi-\eta)) \\ z(\varphi) = -x(\varphi)\,\mathrm{tg}\,\gamma_a + \dfrac{-E + \sqrt{\rho_p^2 - y^2(\varphi)}}{\cos\gamma_a} \end{cases} \quad (11)$$

$$E = \sqrt{\rho_p^2 - \frac{s_a^2}{4}} - R_a\cos\eta_a\sin\gamma_a \quad (12)$$

The radius of the arbitrary M edge point results for φ_y, $0 < \varphi_y < \sqrt{\dfrac{R_a^2}{R_b^2} - 1}$, with

$$R_y = R_b\sqrt{1+\varphi_y^2} \quad (13)$$

It should be noted that the considered M edge point is incident to the MM_1 helix segment. Projecting it along the mentioned helix line, it will meet the plane $z = 0$ in point L. This is the corresponding tool tooth profile point. If projecting the discussed M point along the z- axis in the plane $z = 0$, point K results; this is the point of the tool's generating profile. In case of a new shaper cutter this is incident to the theoretical perfect involute. The profile deviation is measured with the length of arch KL, on the R_y radius circle. Knowing the helix parameter value, $p = R_b / tan\alpha_l$, arch KL results as:

$$KL \equiv \delta_y = \frac{z(\varphi_y)}{p} R_y \quad (14)$$

Equation (14) shows that the greater the z-coordinate values, the greater are the values of the deviation. The z -coordinate's repartition was computed for the simulation setting parameters used before (**Figure 16.**).

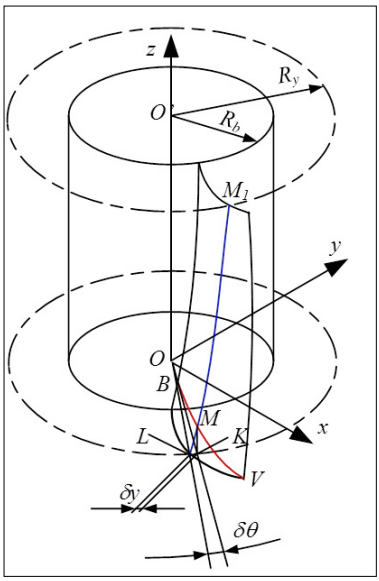

Figure 15. *The tool tooth profile*

It is noted that small cylinder radiuses and axis inclinations lead to z-coordinate values less than 0,2mm. The deviation curves, for different radii and $\gamma_a = 2°$ axis inclination are shown in **Figure 17.**

The shape and the position of the four curves permit the formulation of the following remarks:

– the deviation increases with the radius of the cylinder;

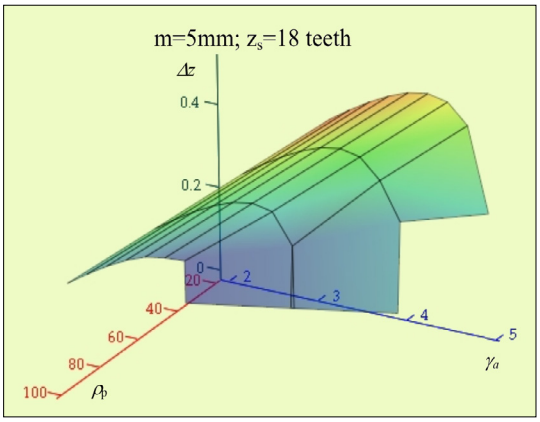

Figure 16. *The repartition of the maximum values of the z-coordinates*

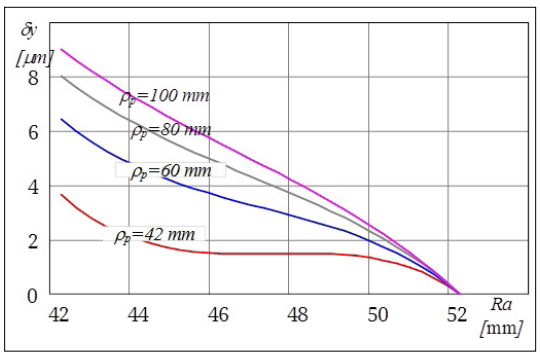

Figure 17. *The deviation curves*

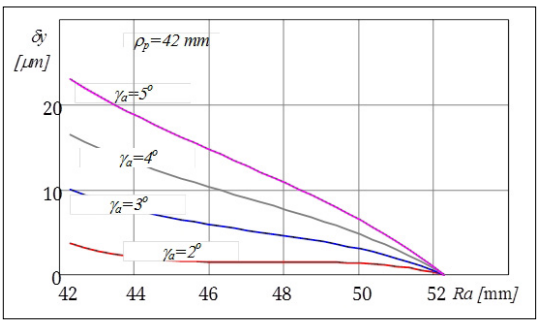

Figure 18. *The variation of the deviation with the inclination of the axis*

– the deviation value is always zero in the edge tip, because this point is included in the plane $z = 0$;

– the largest deviation value is among 9 μm – considered as unacceptable;

– the deviation in case of the smallest radius value is under 4 μm, considered acceptable.

For the constant $\rho_p = 42$ mm, radius and different axis inclinations, **Figure 18.** shows how the deviation increases

Conclusions

The use of the individual cylindrical rake face instead the common conical rake face brings a lot of advantages. The most important of these is the possibility of setting the lateral rake angle value.

But the variation of the rake angle along the cutting edge cannot be set freely: the smaller the cylinder radius, the greater the amplitude of the variation interval. Thus, small inclinations and big radii are advantageous.

On the other hand, on the basis of **Figure 17** and **18.**, it can be concluded that the shaper cutter can be grinded using a straight line profiled grinding wheel, only if the setting region meets small radii and inclination angles, and if accepting small profile errors. The shaper cutter tooth height is constant.

If the errors are not acceptable, relief faces must be grinded with the use of a curved profile grinding wheel.

Acknowledgement

This research was realized with the help of the Domus-fellowship, accorded by the Hungarian Academy of Sciences.

References

[1] Radzewich S. P.: *Gear Cutting Tools*. CRC Press, NY, 2010.

[2] Máté M.: *Hengeres fogaskerekek gyártószerszámai*. Erdélyi Múzeum-Egyesület, 2016.

[3] Máté M., Hollanda D., Forgó, Z., et.al.: *Synthesis of a Profile Errorless Involute Shaper Cutter with Cylindrical Rake Face.* CINTI-MACRO 2019, Konferenciakötet, megjelenés alatt.

[4] Chung-Biau Tsay Wen, Yao Liu Yi-Cheng Chen: *Spur gear generation by shaper cutters.* Journal of Materials Processing Technology, 104/3. (2000) 271–279.

[5] Máté M., Kántor A., Laczkó-Benedek B.: *Metszőkerékkel lefejtett fogaskerekek profilpontosságának vizsgálata.* Műszaki Tudományos Közlemények, 7. (2017) 279–282. https://doi.org/ 10.33895/mtk-2017.07. 62

[6] Zhou Yuansheng, WuYuanhang, Wang Liming, Tang Jinyuan, Ouyang Hongwuab: *A new closed-form calculation of envelope surface for modeling face gears*. Mechanism and Machine Theory, 137/ July (2019) 211–226.

[7] Máté M.: *A possible modelling of the constructive cutting geometry of the gear hobs*. In: Proceedings of the 4-th International Scientific Conference on Advances. Mechanical Engineering. Debrecen, Magyarország. 2016.

[8] Máté M., Hollanda D.: *A hengeres fogaskerék-lefejtő csigamaró működő élgeometriájának vizsgálata.* In: A XVII. Műszaki Tudományos ülésszak előadásai. Műszaki Tudományos Közlemények 6. (2017) 115–120. https://doi.org/10.33895/mtk-2017.06.15

[9] Balajti Zs.: *Examination and adjustment of the bearing pattern in case of helicoid drives.* 8th CIRP Conference on High Performance Cutting, Budapest, Hungary, June 25-27. 2018. Procedia CIRP, appearance is in progress

[10] Forgó Z., Kakucs A., Máté M., Tolvaly-Roşca F.: *Development of Helical Teethed Involute Gear Meshed with a Multi-Edge Cutting Tool Using a Mixed Gear Teeth Modeling Method*. Elsevier Procedia Engineering, 181. (2017) 1–60. https://doi.org/10.1016/j.proeng.2017.02.421

[11] Dudás I.: *The Theory & Practice of Worm Gear Drives.* Kogan Page US, Sterling, USA, ISBN 1 9039 96619 9, 2004.